

Nanoscale

Accepted Manuscript

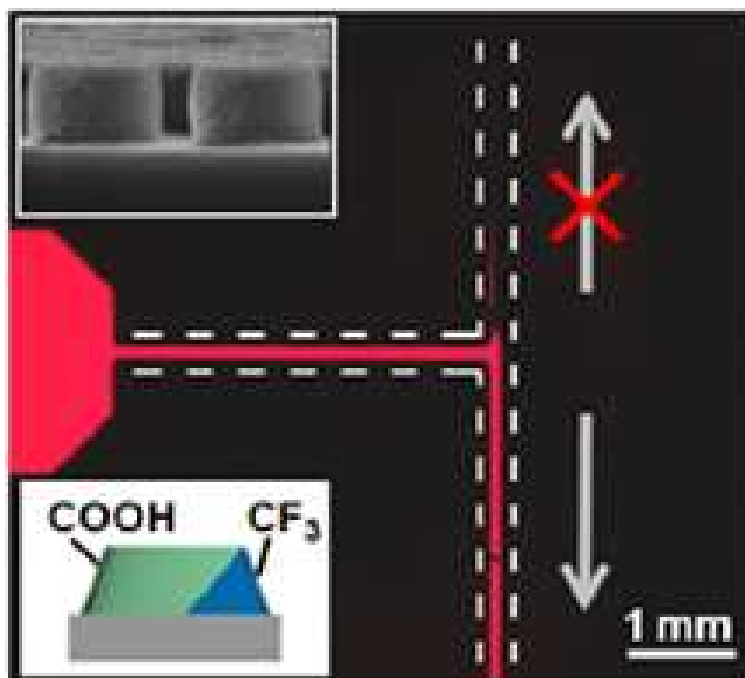


This is an *Accepted Manuscript*, which has been through the Royal Society of Chemistry peer review process and has been accepted for publication.

Accepted Manuscripts are published online shortly after acceptance, before technical editing, formatting and proof reading. Using this free service, authors can make their results available to the community, in citable form, before we publish the edited article. We will replace this *Accepted Manuscript* with the edited and formatted *Advance Article* as soon as it is available.

You can find more information about *Accepted Manuscripts* in the [Information for Authors](#).

Please note that technical editing may introduce minor changes to the text and/or graphics, which may alter content. The journal's standard [Terms & Conditions](#) and the [Ethical guidelines](#) still apply. In no event shall the Royal Society of Chemistry be held responsible for any errors or omissions in this *Accepted Manuscript* or any consequences arising from the use of any information it contains.



One-way valve of microfluidic system is fabricated through introducing Janus Si pillar arrays with outstanding anisotropic wettability into the T-shaped microchannel. The one-way valve shows great ability to guide the fluid flow and to separate gas from liquid in MF systems, which make the one-way valve competitive candidate for further improvement of MF systems.

ARTICLE

Anisotropic Janus Si Nanopillar Arrays as a Microfluidic One-Way Valve for Gas-Liquid Separation

Cite this: DOI: 10.1039/x0xx00000x

Received 00th January 2012,
Accepted 00th January 2012

DOI: 10.1039/x0xx00000x

www.rsc.org/

Tieqiang Wang,^{a,c} Hongxu Chen,^a Kun Liu,^a Yang Li,^b Peihong Xue,^a Ye Yu,^a
Shuli Wang,^a Junhu Zhang,^{*a} Eugenia Kumacheva^{*b} and Bai Yang^a

In this paper, we demonstrate a facile strategy for the fabrication of one-way valve for microfluidic (MF) systems. The micro-valve was fabricated by embedding arrays of Janus Si elliptical pillars (Si-EPAs) with anisotropic wettability into a MF channel fabricated in poly(dimethylsiloxane) (PDMS). Two sides of the Janus pillar are functionalized with molecules with distinct surface energies. The ability of the Janus pillar array to act as a valve was proved by investigating the flow behaviour of water in a T-shaped microchannel under different flow rates and pressures. In addition, the one-way valve was used to achieve gas-liquid separation. We believe that the Janus Si-EPAs modified by specific surface functionalization provide a new strategy to control the flow and motion of fluids in MF channels.

Introduction

In the past decade, microfluidics (MFs) has shown promising applications in chemistry and biochemistry, owing to reduced reagent consumption, shortened analysis time, high sensitivity, portability and low cost.¹⁻⁹ Nevertheless, some technical challenges limit practical applications of MF devices. One of the technical difficulties includes control of the motion of fluids in microchannels, which requires the use of micro-valves.¹⁰⁻¹⁴ Applications of micro-valves include flow regulation, on/off switching and sealing of liquids, gases or vacuum. Although a variety of miniaturized mechanical valves and pneumatic-controlled valves have been fabricated by micro-manufacture technologies,^{4,15-17} all of them require the fabrication and construction of mechanical moving parts or external control parts in the channel, which increases the cost and size of the integrated MF device. To overcome this drawback, non-mechanical materials-based valves have been introduced, which utilized a reversible volume change of the materials, due to the change of temperature, pH or phase transition of the surrounding solution.¹⁸⁻²⁰ These non-mechanical methods require changes of the chemical or physical environments for the liquid, which limits their applications in MF devices. Thus, the development of alternative cost-efficient non-mechanical micro-valves is highly desirable.

In a microchannel, the flow behaviour of a fluid is strongly affected by the surface properties of the surrounding walls, due to the large surface-to-volume ratio. Thus, tuning of the wettability of the walls may lead to another strategy in controlling fluid flow.¹⁴ For example, anisotropic wetting surfaces, such as the gradient surface and stooped nanohairs, can result in inhomogeneous distribution of liquid on the

surface and provides the capability to guide liquid flow in a particular direction.²¹⁻²³ Although control of fluid flow by modifying the wettability of microchannels has been reported by many research groups,²⁴⁻³⁶ the number of works utilizing surfaces with anisotropic wetting properties to enhance the fluid control in microchannels is limited.³⁷⁻³⁹ In addition, to the best of our knowledge, micro-valves utilizing anisotropic wetting surfaces have not been reported.

Recently, we have reported the utilization of two-dimensional (2D) elliptical hemisphere arrays (EHAs) of polystyrene as a mask to fabricate silicon elliptical pillar arrays (Si-EPAs), which were used for the fabrication of Janus Si pillar arrays with unique anisotropic wettability.⁴⁰ In the present work, we report the application of these arrays as a one-way valve for MF systems. The one-way valve was fabricated by integrating a poly(dimethylsiloxane) (PDMS) channel with the Janus Si-EPAs. The ability of the Janus array to function as a valve was demonstrated by investigating the flow of an aqueous solution in the MF channel. By examining the fluid motion under different flow rates (2.0-8.0 $\mu\text{L min}^{-1}$) and pressures (26-83 mbar), we found that the Janus Si-EPAs performed similarly to the closed elastomeric membrane valve.¹⁷ In addition, we investigated how the size of the MF channels and the geometry of the Janus Si-EPAs affect valve performance. Finally, the applications of the one-way valve were demonstrated for the separation of gas from water in the microchannel.

Experimental section

Materials

Silicon and glass substrates were cleaned by immersion in piranha solution (3:1 concentrated $\text{H}_2\text{SO}_4/30\% \text{H}_2\text{O}_2$) for 1 h at 70 °C to create a hydrophilic surface and then rinsed repeatedly with Milli-Q water ($18.2 \text{ M}\Omega \text{ cm}^{-1}$) and ethanol. The substrates were dried in nitrogen gas before use. PDMS elastomer kits (Sylgard 184) were purchased from Dow Corning (Midland, MI). 16-Mercaptohexadecanoic acid (MHA), Trichloro (1H,1H,2H,2H-perfluorooctyl) silane (PFS) and Polystyrene (PS) ($M_w=280,000$) were all purchased from Aldrich. Sulfuric acid and hydrogen peroxide were used as received. The “T-shaped” and “cross-shaped” glass MF chips were obtained from Key lab of Analytical Chemistry for Life Science Nanjing University. The MF chip used for gas-liquid separation was fabricated through photolithography.

Preparation

PS elliptical hemisphere arrays were first fabricated through a micromolding method and used as the etching mask for the preparing of Si elliptical pillar arrays.⁴¹ To fabricate Janus Si-EPAs, the elliptical pillar frameworks were firstly modified with PFS through chemical vapor deposition. Then, through oblique thermal evaporation of gold, one side of all elliptical pillars was deposited with a thin film of Au (about 20 nm). Selective modification of MHA onto Au surface was performed through immersing the Janus array into an ethanol solution of MHA with concentration of about 4 mM. As a control sample, the frame work of the cylindrical sample was Si cylinder arrays etched from PS round hemisphere arrays which was fabricated based on the same micromolding strategy without ovalization of the mold. To fabricate PDMS MF channel, PDMS prepolymer was first casted onto the glass MF chip, after the PDMS prepolymer were cured in a conventional drying oven at 60 °C for 3 h, the PDMS MF channel was peeled off from the MF chip. After the PDMS channel was connected with an automatic sample injector using a PTFE pipe, the PDMS channel was compressed onto the surface of the Janus Si-EPAs to fabricate the MF one-way valve based on the as-prepared Janus arrays.

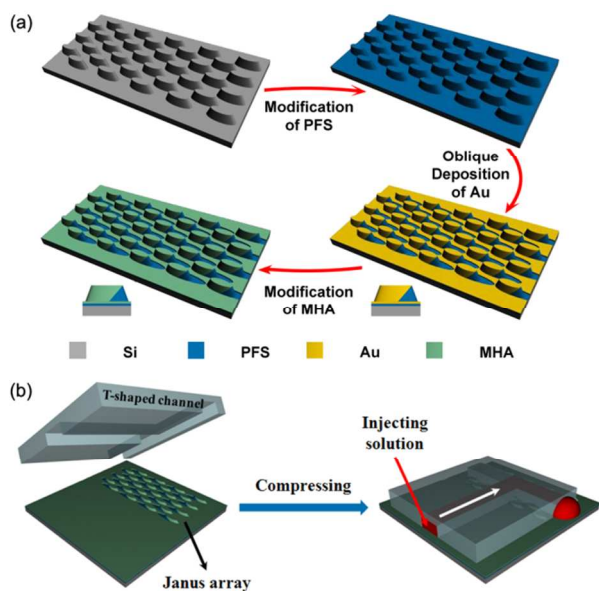


Figure 1. (a) The schematic illustration of the procedure for the fabrication of the PFS-MHA Janus Si pillar arrays. (b) The schematic illustration of the fabrication process of the one-way valve for MF system.

Characterization

Scanning electron microscopy (SEM) micrographs were taken with a JEOL FESEM 6700F electron microscope with primary electron energy of 3 kV. Before imaging, the samples with polymer structures were sputter-coated with 2 nm of Pt. The chemical compositions were determined by X-ray photoelectron spectroscopy (XPS, Thermo ESCALAB 250). The wetting behavior of water droplet on the surface of Janus array was recorded using a drop shape analysis system (DSA 10 MK2, KRÜSS). The running behavior of Rhodamine B aqueous solution in the MF channel was recorded with an Olympus fluorescence microscope (BX51). The water pressure in the MF channels was measured using Microfluidic Flow Control System (MFCS and FLOWELL, FLUIGENT).

Results and discussions

Fabrication of the Janus Si elliptical pillar arrays

Figure 1 shows the preparing procedure of the Janus Si-EPAs (Figure 1(a)) and the Janus array-based MF one-way valve (Figure 1(b)). Briefly, the Si-EPAs were fabricated via an etching method by using PS-EHAs etching masks, which were prepared by a micromolding method.^{40,41} The scanning electron microscopy (SEM) image of the as-prepared Si-EPA clearly shows the elliptical shape of the Si pillars (Figure 2(a)). The average height of the pillars was about 504 nm (Figure 2(b)). The surface of the Si-EPAs was modified with a thin layer of hydrophobic trichloro (1H,1H,2H,2H-perfluorooctyl) silane (PFS) molecules by using chemical vapor deposition. The peak at 684 eV (F_{1s}) in the X-ray photoelectron spectroscopy (XPS) spectrum of the modified Si-EPAs (Figure 2(c)) explicitly indicates that the PFS molecules were bonded onto the Si surface. Next, a thin layer of Au was obliquely deposited onto

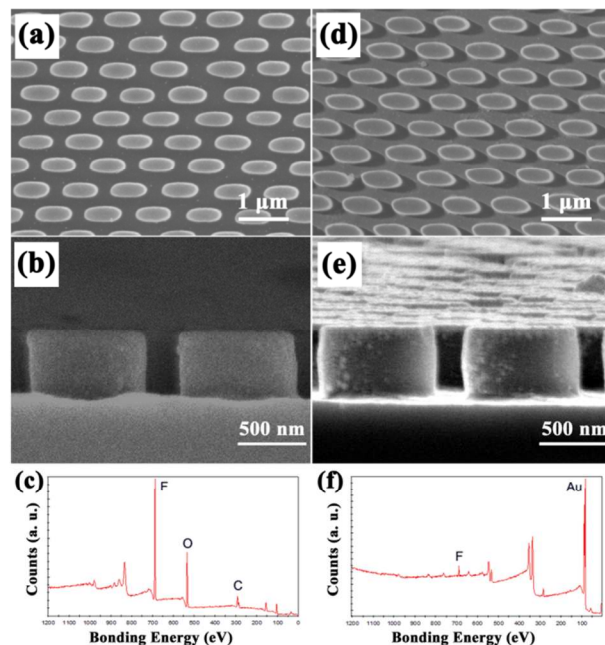


Figure 2. The SEM images of (a) the fabricated silicon pillar array and (d) the as-prepared PFS-MHA Janus arrays. (b) and (e) are the cross-section SEM images taken along the short axis direction of the elliptical pillar array of the sample shown in (a) and (d), respectively. The XPS spectrum of (c) the PFS-modified silicon pillar array and (f) the as-prepared Janus arrays before the MHA modification.

the Si-EPA surface by thermal evaporation, as shown in Figure 2(d). A cross-section SEM examination of the modified Si-EPAs proved the Janus nature of the Si pillar arrays, that is, one side of each Si pillar was covered by gold while almost no gold was deposited on the other side (Figure 2(e)). In addition, the presence of the F_{1s} peak at 684 eV in the XPS spectrum for the modified Si-EPAs also suggested a partial coverage of gold on the Si pillars (Figure 2(f)). Finally, a self-assembled monolayer of hydrophilic 16-mercaptohexadecanoic acid (MHA) molecule was selectively attached on the top of the gold layer by using covalent bonding between Au and the thiol group of MHA. Additionally, as shown in the XPS spectrum of the PFS-MHA Janus pillar array (Figure S1), the F_{1s} peak still exist while the S_{2p} peak also appears at 164 eV, this clearly indicate that the hydrophilic MHA molecular was selectively attached on the top of the gold while the other area was still modified by hydrophobic PFS molecular. Following this procedure, one side of the Si pillars was covered with a hydrophobic PFS layer, and the other side of the pillars was covered with a hydrophilic MHA layer, thereby rendering a Janus nature of the pillars.

Wetting behaviour of the Janus Si pillar arrays

Because of the Janus structure, the modified Si-EPAs were expected to exhibit anisotropic wettability, which was examined by studying the wetting behavior of water on the surface. Figure 3 shows the photographs of a 20- μ L water droplet, which were taken at different time intervals after the droplet contacted the surface of the arrays. The photographs were taken along the direction perpendicular to the evaporating direction of gold. The sample shown in Figure 3(a-d) was fabricated by evaporating gold along the long axis of the elliptical pillar (abbreviated as the long-axis-sample), while Figure 3(e-h) shows the photographs of the sample fabricated by evaporating gold along the short axis of the elliptical pillar (abbreviated as the short-axis-sample). As the water was

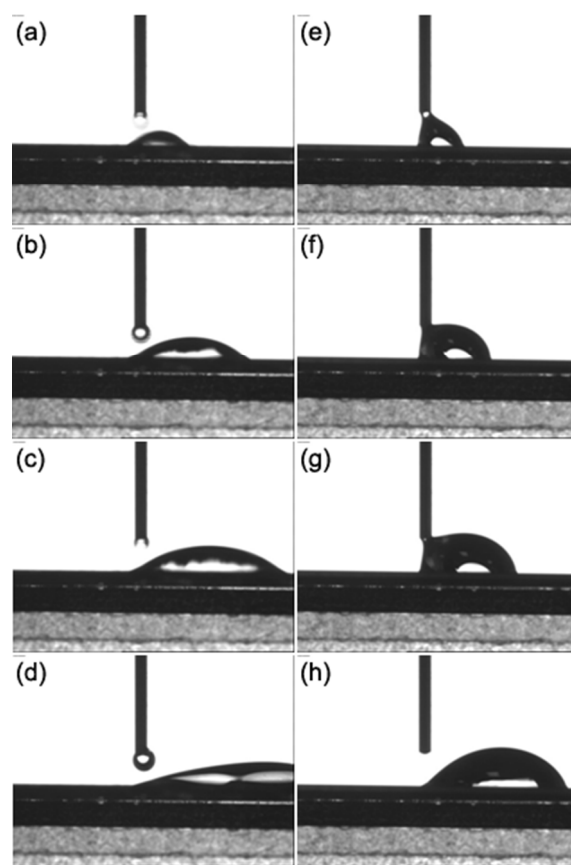


Figure 3. Photographs of the water drop taken at different time after the water drop contacted the surface of Janus array of (a-d) the long-axis-sample and (e-h) the short-axis-sample. The MHA-modified direction was placed at the right side when taking photographs.

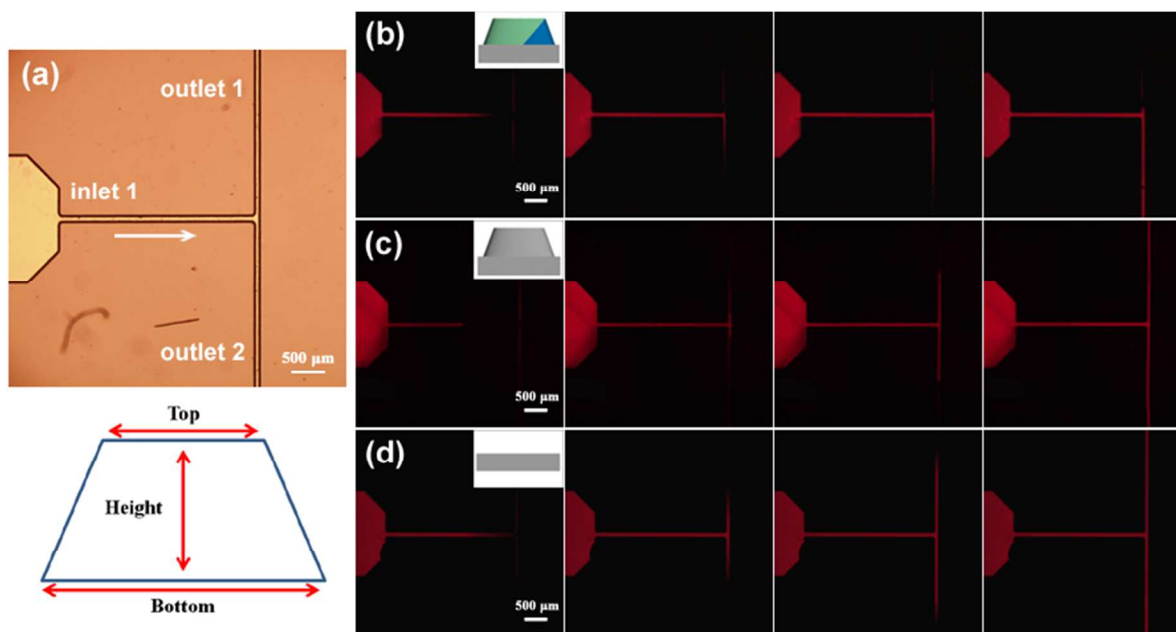


Figure 4. (a) The optical microscope image of the T-shaped MF channel and a schematic illustration of the sectional profile of the channel (inlet: height = 38 μ m, top = 65 μ m, bottom = 120 μ m; outlet: height = 36 μ m, top = 18 μ m, bottom = 65 μ m). The white arrow represents the injecting direction of the water. (b-d) the flow behavior of the Rhodamine aqueous solution in the T-shaped MF channel bounding (b) the PFS-MHA Janus pillar array, (c) Si pillar array without asymmetric modification and (d) planar Si substrate, the inset is the schematic illustration of the bottom geometry of the microchannel. The time point of (b), (c) and (d) is about 0 s, 2 s, 4 s, and 7 s from left to right. The scale bars are 500 μ m and the downward direction is the MHA-modified direction. The red threads near the T-junction result from the reflection of ambient light against the side wall.

continuously injected into the water droplet on the surface of the Janus arrays, the three-phase contact line only moved towards the MHA-modified direction, while the contact line at the PFS-modified side was pinned on the surface. Owing to distinct surface energies of the molecular modified on two sides of the Janus pillars, the advancing angle of water on such surface was anisotropic, thereby leading to anisotropic spreading of water.

Although the wetting behaviours of water on both samples were anisotropic, they are obviously different. Anisotropic wetting on the long-axis-sample was significantly faster than that of the short-axis-sample, and the advancing angle of the former was smaller than that of the latter. We ascribe this difference to the lower energy barrier for the water to wet the surface along the long-axis-direction than that along the short-axis-direction.⁴⁰ Therefore, the speed of wetting for the long-axis-sample was substantially larger than that of the short-axis-sample. In addition, the degree of coverage of the pillar with gold was also higher for the long-axis-sample (Figure 2(b) and Figure (S2)). Thus, the ratio of the hydrophilic area-to-hydrophobic area was larger for the long-axis-sample, which could contribute to the higher speed of anisotropic wetting. To facilitate the discussion of the valve function of the as-prepared Janus array, unless specified, we describe the pillars coated with gold along their long axis in the rest of the paper.

Fabrication of the one-way valve based on the Janus Si pillar arrays

In order to explore potential applications of the Janus Si pillar array in MF devices, a T-shaped microchannel fabricated in PDMS was integrated with the Janus Si-EPAs to build a one-way valve (Figure 1(b)). In brief, the T-shaped PDMS channel was cast on a glass MF molds. After being cured and peeled off, the T-shaped PDMS micro-channel was compressed against the surface of the Janus Si-EPA, so that the Janus array was positioned at the T-junction. To observe the fluid motion in the microchannel, an aqueous solution of fluorescent Rhodamine dye was used. Figure 4(a) shows the optical microscopy image of the T-shaped MF channel. The solution was introduced in inlet 1 through small PTFE tubing connected to an automatic sample injector under a flow rate of $2.0 \mu\text{L min}^{-1}$. The outlets were all connected to the atmosphere. Under this condition, the driving pressure was ~ 26 mbar. Figure 4(b) shows the flow behaviour of the Rhodamine aqueous solution in the T-shaped MF channel bound to the PFS-MHA Janus pillar array. The aqueous solution was directed to the outlet 2 channel (the hydrophilic MHA-modified direction), while a very small amount of the solution flowed into but stopped in the outlet 1 channel (the hydrophobic PFS-modified direction). The corresponding video of the Rhodamine solution flowing in the T-shaped channel is given in Electronic Supplementary Information (Video S1). These results revealed that the fluid motion into the outlet 1 channel was largely suppressed and the Janus Si pillar array served as a one-way valve in the microchannel. Since the interaction between the aqueous solution and the hydrophobic PDMS surface is very weak, we believe that it is the anisotropic wettability of the Janus Si-EPAs surface that induces the anisotropic flow behavior of water in the T-shaped MF channel. We note that during the entire process no external pressure was exerted on the outlet 1 channel, which allowed us to avoid the utilization of the costly and bulky external flow control parts. In the control experiments, we tested the flow behaviour of the Rhodamine aqueous solution in the T-shaped MF channel bounding Si


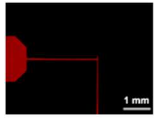
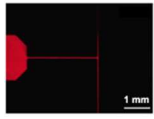
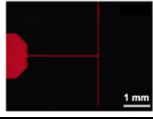
pillar array without asymmetric modification and planar Si substrate (Figure 4(c-d)). We found that the solution readily moved in both directions of the T-shaped channel, which suggested that these two surfaces did not guide the direction of flow in the MF channel.

To further demonstrate the valve performance of the Janus Si pillar arrays, we used a cross-shaped MF channel. Owing to the anisotropic wettability of the Janus array, the aqueous Rhodamine solution moved into the outlet 2 channel (the MHA-modified direction), while the other two outlets channels were “closed” (Figure S3).

Examination of valve performance of the Janus arrays

To further investigate the performance of the valve based on the Janus Si-EPA, we examined the motion of the aqueous solution moving in the T-shaped channel under different flow rates (Table 1). Table 1 shows the fluorescence microscopy images that were captured when the aqueous solution flow out of vision of the microscope. In addition, according to the fluorescence images, the ratio of the flowing distance of aqueous solution along the PFS-modified direction to that along the MHA-modified direction ($D_{\text{PFS}}/D_{\text{MHA}}$) was used to characterize the valve performance of the Janus Si-EPAs (the relationship between the flow rate and $D_{\text{PFS}}/D_{\text{MHA}}$ is also given in Figure S4, the higher this ratio was, the better the Janus array based valve performed). When the flow rate was $2.0 \mu\text{L min}^{-1}$, the driving pressure used was relatively low (26 mbar). The ratio $D_{\text{PFS}}/D_{\text{MHA}}$ was close to zero, indicating that the Janus array efficiently functioned as a one-way valve. When the flow rate increased to $3.0 \mu\text{L min}^{-1}$, the driving pressure of the liquid increased from 26 to 35 mbar, a small amount of the solution entered into and stopped in the outlet 1 microchannel (the PFS-modified direction). This result suggested that as the driving pressure became higher, the flow of liquid in the PFS-modified direction of flow was not completely suppressed. When the flow rate increased further from 3.0 to $8.0 \mu\text{L min}^{-1}$ (corresponding to the increase in driving pressure from 35 to 83 mbar), the channel along the PFS-modified direction gradually

Table 1. The detail flowing parameters of the aqueous solution in the T-shaped channel under different flow rates. The scale bars are 1 mm and the downward direction is the MHA-modified direction.

Flow Rate ($\mu\text{L min}^{-1}$)	Flow Speed (m min^{-1})	Driving Pressure (mBar)	Fluorescence Images	$D_{\text{PFS}}/D_{\text{MHA}}$
2.0	0.57	26		0
3.0	0.85	35		0.08 ± 0.06
4.0	1.14	45		0.37 ± 0.12
8.0	2.28	83		0.98 ± 0.10

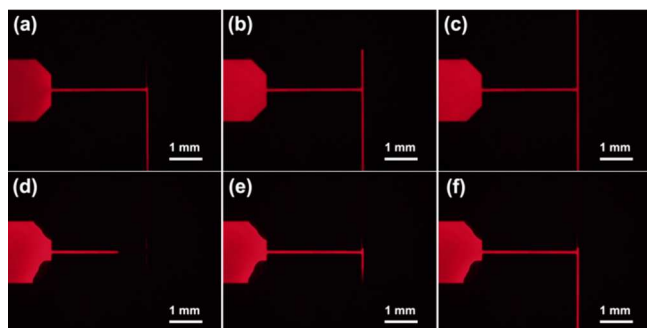


Figure 5. (a-c) The fluorescence microscope images of the Rhodamine aqueous solution when the liquid pressure begins to increase from that lower than failure pressure (~ 20 mbar) to that higher than failure pressure (~ 60 mbar). (d-f) The fluorescence microscope images of the Rhodamine aqueous solution injected into the microchannel under pressure of ~ 20 mbar after the aqueous solution was ejected by air. The scale bars are 1 mm and the downward direction is the MHA-modified direction.

opened. When the flow rate was above $8 \mu\text{L min}^{-1}$, the channel in the PFS-modified direction was completely open for the Rhodamine solution. These results imply that in the particular pressure range the Janus arrays could serve as a valve similar to the closed elastomeric membrane valve reported before.^{10,17} As concluded in Table 1, there exist a threshold pressure (failure pressure) for this one-way valve performance. Since the main driving force of the directional flow is the surface tension difference between two opposite directions, we believe that the main reason for the failure of the as-prepared one-way valve is the excess of the liquid pressure. If the driving force of the aqueous solution is much smaller than the surface tension difference, the aqueous will flow along the MHA-modified direction, however, if the driving force exceeds the surface tension difference, the directional flow of aqueous solution will failed. Additionally, there are still some other minor reasons for the failure of the valve, such as the deformation of the PDMS,^{42,43} and the fluctuations of the driving pressure, utilization of undeformable glass material to fabricate the microchannel or stabilizing the driving pressure may be some possible approach for the improvement of the valve performance.

Next, we performed a close-open-close procedure of the valve by varying the driving pressures from 20 to 60 mbar, and subsequently decreasing it to 20 mbar. Figure 5 shows the fluorescence images of the aqueous solution in the T-shaped microchannel during a close-open-close cycle (the MF channel was the same as that shown in Figure 4(a)). When the driving pressure was relatively low (~ 20 mbar), the Janus arrays served as a one-way valve well (Figure 5(a)). After the pressure was increased above the failure pressure of ~ 60 mbar, the outlet 1 channel opened and the Rhodamine solution flowed into the outlet 1 channel (Figure 5(b-c)). To close the outlet 1 channel,

Table 2. The detail flowing parameters of the aqueous solution in T-shaped channel with different dimensions when the Janus array failed to function as a one-way-valve.

Channel No.	Horizontal Channel (μm)			Perpendicular Channel (μm)			Flow Rate ($\mu\text{L min}^{-1}$)	Flow Speed (m min^{-1})	Pressure (mBar)	PF/BH ($\text{mBar } \mu\text{m}^{-1}$)	PF/BP ($\text{mBar } \mu\text{m}^{-1}$)
	Top	Bottom	Height	Top	Bottom	Height					
No. 1	85	140	38	35	85	36	6.0	1.51	45	0.540	0.321
No. 2	65	120	38	18	65	36	3.0	0.85	35	0.538	0.291
No. 3	55	110	38	10	63	36	1.5	0.48	32	0.507	0.290

P_F represents the failure pressure; B_H represents the bottom size of the horizontal channel; B_P represents the bottom size of the perpendicular channel.

Table 3. The detail flowing parameters of the aqueous solution in No. 2 T-shaped channel when the Janus array failed to function as a one-way-valve for samples with different geometries.

Sample	Flow Rate ($\mu\text{L min}^{-1}$)	Flow Speed (m min^{-1})	Failure Pressure (mBar)
short-axis-sample	8.0	2.28	83
long-axis-sample	3.0	0.85	35
cylindrical sample	4.0	1.14	45

the driving pressure of the aqueous solution was reduced to ~ 20 mbar. Under this condition, the directional flow of the solution was recovered, and the outlet 1 channel was “closed” again (Figure 5(d-f)).

Since the failure pressure is a critical parameter for the Janus arrays to serve as one-way valve of MF system, we studied the factors affecting the failure pressure (see Table 2 and Table 3). Table 2 shows the detailed flow characteristics in a T-shaped channel with different dimensions, for which the Janus array failed to function as a one-way valve. The corresponding dimensions of T-shaped channels are also listed in Table 2 (from channel #1 to channel #3, the sectional area of the channel gradually decreased). The results given in Table 2 reveal that a higher failure pressure was characteristic for microchannels with larger dimensions. We assume this effect was attributed to the larger bottom surface area of the microchannel, that is, a larger number of the Janus pillars in the channel. In addition, as shown in Table 2, the numerical ratio between the failure pressure and the bottom width of channel for the microchannels with different dimensions is nearly constant. The variation of the failure pressure with the bottom width of the channel also showed that this ratio was independent of the width of the bottom surface of the channel (Figure S5). Furthermore, we have fabricated Janus pillar arrays with half density of pillars through combining our colloidal lithography method and photolithography method, as shown in figure S6. It was found that the failure pressure of this sample (~ 15 mbar) is really much smaller than that of the Janus array with higher density of pillars. This could to some extent prove this assumption. Moreover, Table 3 shows the characteristic flow conditions under which the Janus array based valve failed to direct solution flow in a particular direction for the same T-shaped channel (channel #2) integrated with one of three types of arrays, namely, the short-axis-sample, the long-axis-sample and the cylindrical sample (the cylindrical sample was a control sample, and its detail fabricating process was shown in the preparation section). Based on the results given in Table 3, we

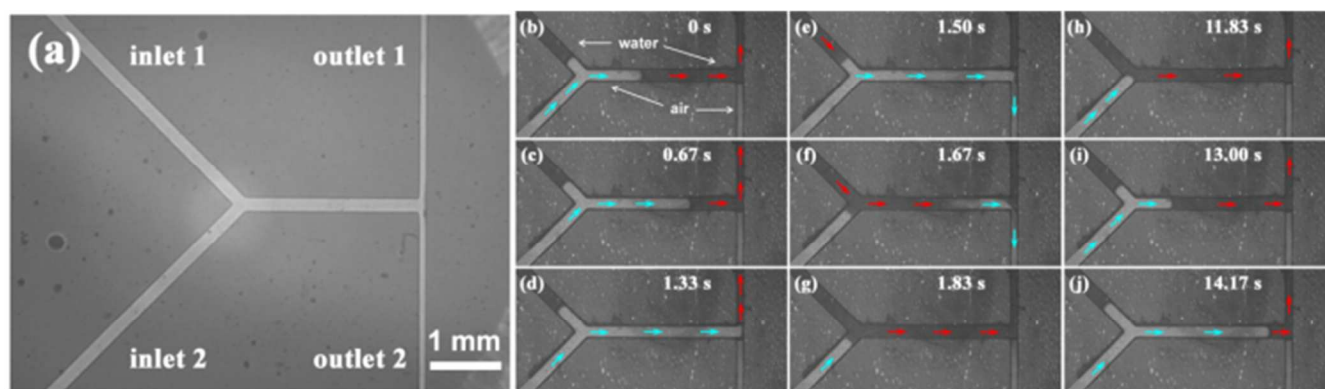


Figure 6. (a) The microscope image of the MF channel used for gas-liquid separation. The microscope images of the MF channel (b-d) before and (e-g) after the air plugs passed the T-shaped junction. (h-j) The microscope images of the MF channel before next air plugs arrived the T-shaped junction. The dark part represents water and the light part air. The red arrows represent the flow direction of water and the cyan arrows represent the flow direction of air. The scale bar of (a) is also suitable for (b-j) and the upward direction is the MHA-modified direction.

conclude that the short-axis-sample possessed the highest failure pressure, while the long-axis-sample exhibited the lowest failure pressure. Because the wetting energy barrier along the anisotropic wetting direction increased in a sequence long-axis-sample \sim cylindrical sample \sim short-axis-sample, the wetting along the MHA- and PFS-modified directions became more difficult from the long-axis-sample to the short-axis-sample. We believe that it is a larger energy barrier for the wetting along the PFS-modified direction of the short-axis-sample that caused a higher failure pressure for this sample.

Although the maximum water pressure for the Janus array to serve as an efficient one-way valve was not high, the flow rate in the range below $3 \mu\text{L min}^{-1}$ is sufficient for many MF applications. Moreover, the effective area of the Janus array is only tens of square micrometers in the T-junction, indicating that the array has sufficient ability to direct the flow of water in MF channels. Additionally, it does not mean that the higher is the better, if one wants to adjust the flowing condition of fluid through a relative low pressure change, the valve with lower threshold pressure would be a better candidate.

Gas-liquid separation in the microchannel based on the as-prepared one-way valve

Typically, gas-liquid and liquid-liquid multiphase chemical reaction may require the separation of different fluid phases from each other for further analysis or processing. In MF systems, such separation is challenging, due to the difficulty in handling small volumes of fluid. Currently, the separation of two immiscible fluid phases is mainly achieved by using gravity,⁴⁴ capillary force,^{45,46} and Laplace force.⁴⁷ Here, we tested gas-liquid separation on the Janus Si-EPA one-way valve. Figure 6(a) shows an optical microscopy image of the MF bubble generator combined with the T-junction microchannel used for gas-liquid separation. An aqueous solution and air were injected from the inlet 1 and inlet 2 of the Y-junction of the MF channel, respectively. The flow rate of aqueous solution and air is $1 \mu\text{L min}^{-1}$ and $30 \mu\text{L min}^{-1}$, respectively. Water slugs and air plugs formed at the Y-junction and moved to the one-way valve T-junction integrated with the Janus array. When the aqueous solution reached the T-junction, owing to the anisotropic wettability of the Janus arrays, the one-way valve directed the flow of water slugs only into the outlet 1 channel (the MHA direction), as shown in Figure 6(b-d). When an air plugs arrived to the T-junction, the outlet 1 channel was filled with the aqueous solution, while the outlet 2

channel was open. Thus, the hydrodynamic resistance for the flow of the air plug in the outlet 1 channel was significantly higher than that for outlet 2 channel, and the air plugs only entered the outlet 2 channel, thereby separating themselves from the water slugs (Figure 6(e-g)). The separation of the air plugs and water slugs into different outlet channels is clearly shown in Figure S7. After the air plug moved out of the outlet 2 channel, owing to the existence of the one-way valve, the adjacent water slug moved into the outlet 1 channel, until the next air plugs arrived (Figure 6(h-j)). The corresponding video of the entire gas-liquid separation process is given in Electronic Supplementary Information (Video S2). Since these two fluid phases are immiscible with each other, thus, we have observed outlets carefully under higher magnification. We found that there is little air bubble existing in the liquid phase, and there is also no water slugs found in the air phase, thus, we believe that the purity of these two phases is nearly 100% after flow out of the microfluidic channel. These results show that the one-way valve based on the Janus arrays can be successfully used for gas-liquid separation.

Conclusions

In summary, we developed a one-way valve in the MF system based on the array of Janus Si pillars with anisotropic surface wetting behaviour. The performance of the valve was evaluated in channels with different dimensions, for different driving flow rates and pressure of water and for pillars with varying geometries. Gas-liquid separation was also successfully performed based on the Janus Si-EPA one-way valve. Because no complicated external control parts are used, the Janus Si-EPA valve is a competitive candidate for further developments of MF systems. Moreover, as the performance of the valve originates from the distinct surface energies of two sides of the Janus Si pillars, the separation of other immiscible phases, such as oil-water, in MF channels would also be expected through modifying two sides of the Janus pillar with oleophobic and oleophilic functional groups. We note that the proposed valve is passive: the design and valve performance does not change from experiment to experiment. We anticipate that smart valves based on Janus Si pillar arrays can be produced based on selective modification of photo or thermo-responsive materials, which should show a broad range of applications in future MF systems.

Acknowledgements

This work was supported by the National Basic Research Program of China (2012CB933800), the National Natural Science Foundation of China (Grant Nos. 21222406, 21074048, 91123031, 21221063), Science and Technology Development Program of Jilin Province and the Program for New Century Excellent Talents in University. We thank Prof. J. Xu and Dr. B. Xu from Key lab of Analytical Chemistry for Life Science Nanjing University for the fabrication of the glass MF chip.

Notes and references

^a State Key Laboratory of Supramolecular Structure and Materials, College of Chemistry, Jilin University, Changchun 130012, P. R. China. E-mail: zjh@jlu.edu.cn; Fax: +86-0431-85193423; Tel: +86-0431-85168283.

^b Department of Chemistry, University of Toronto, Toronto, Ontario M5S 3H6, Canada. E-mail: ekumache@chem.utoronto.ca.

^c Research Center for Molecular Science and Engineering, Northeastern University, Shenyang 110004 (P. R. China).

† Electronic Supplementary Information (ESI) available: the XPS spectrum of the as-prepared Janus arrays after the MHA modification; the SEM images of the PFS-MHA Janus Si pillar arrays fabricated through oblique evaporating gold along the short axis of the elliptical pillars; images of the cross-shaped MF channel and Rhodamine aqueous solution injecting in a cross-shaped MF channel taken at different time; the plot data of $D_{\text{PFS}}/D_{\text{MHA}}$ against the flow rate of the aqueous solution; the plot data of failure pressure against the bottom size of the channel; optical microscopy images of the Janus pillar array with less density of pillars; optical microscopy images of the T junction with higher magnification; the video of Rhodamine solution running in the T-shaped microchannel integrated with the Janus Si-EPA; the video of the entire gas-liquid separation process. See DOI: 10.1039/b000000x/.

- 1 G. M. Whitesides, *Nature*, 2006, **442**, 368.
- 2 P. A. Auroux, D. Iossifidis and D. R. Reyes, A. Manz, *Anal. Chem.*, 2002, **74**, 2637.
- 3 D. R. Reyes, D. Iossifidis and P. A. Auroux, A. Manz, *Anal. Chem.*, 2002, **74**, 2623.
- 4 M. S. Thomas, B. Millare, J. M. Clift, D. Bao, C. Hong and V. I. Vullev, *Ann. Biomed. Eng.*, 2010, **38**, 21.
- 5 S. Nagrath, L. V. Sequist, S. Maheswaran, D. W. Bell, D. Irimia, L. Ulkus, M. R. Smith, E. L. Kwak, S. Digumarthy, A. Muzikansky, P. Ryan, U. J. Balis, R. G. Tompkins, D. A. Haber and M. Toner, *Nature*, 2007, **450**, 1235.
- 6 P. S. Dittrich and A. Manz, *Nature*, 2006, **5**, 210.
- 7 L. S. Bouchard, S. R. Burt, M. S. Anwar, K. V. Kovtunov, I. V. Koptuyug and A. Pines, *Science*, 2008, **319**, 442.
- 8 A. P. Esser-Kahn, P. R. Thakre, H. Dong, J. F. Patrick, V. K. Vlasko-Vlasov, N. R. Sottos, J. S. Moore and S. R. White, *Adv. Mater.*, 2011, **23**, 3654.
- 9 A. J. Chung, D. Kim and D. Erickson, *Lab Chip*, 2008, **8**, 330.
- 10 K. W. Oh and C. H. Ahn, *J. Micromech. Microeng.*, 2006, **16**, R13.
- 11 S. E. Hulme, S. S. Shevkoplyas and G. M. Whitesides, *Lab Chip*, 2009, **9**, 79.
- 12 A. V. Desai, J. D. Tice, C. A. Apblett and P. J. A. Kenis, *Lab Chip*, 2012, **12**, 1078.
- 13 F. Benito-Lopez, R. Byrne, A. M. Răduță, N. E. Vrana, G. McGuinness and D. Diamond, *Lab Chip*, 2010, **10**, 195.
- 14 G. Takei, M. Nonogi, A. Hibara, T. Kitamori and H. Kim, *Lab Chip*, 2007, **7**, 596.
- 15 V. Studer, G. Hang, A. Pandolfi, M. Ortiz, W. F. Anderson and S. R. Quake, *J. Appl. Phys.*, 2004, **95**, 393.
- 16 M. A. Unger, H.-P. Chou, T. Thorsen, A. Scherer and S. R. Quake, *Science*, 2000, **288**, 113.
- 17 W. H. Grover, R. H. C. Ivester, E. C. Jensen and R. A. Mathies, *Lab Chip*, 2006, **6**, 623.
- 18 C. Yu, S. Mutlu, P. Selvaganapathy, C. H. Mastrangelo, F. Svec and J. M. J. Frechet, *Anal. Chem.*, 2003, **75**, 1958.
- 19 D. J. Beebe, J. S. Moore, J. M. Bauer, Q. Yu, R. H. Liu, C. Devadoss and B. H. Jo, *Nature*, 2000, **404**, 588.
- 20 L. Gui and J. Liu, *J. Micromech. Microeng.*, 2004, **14**, 242.
- 21 D. Y. Xia, L. M. Johnson and G. P. López, *Adv. Mater.*, 2012, **24**, 1287.
- 22 K. H. Chu, R. Xiao and E. N. Wang, *Nat. Mater.*, 2010, **9**, 413.
- 23 N.A. Malvadkar, M. J. Hancock, K. Sekeroglu, W. J. Dressick and M.C. Demirel, *Nat. Mater.*, 2010, **9**, 1023.
- 24 A. Hibara, S. Iwayama, S. Matsuoka, M. Ueno, Y. Kikutani, M. Tokeshi and T. Kitamori, *Anal. Chem.*, 2005, **77**, 943.
- 25 A. Hibara, M. Nonaka, H. Hisamoto, K. Uchiyama, Y. Kikutani, M. Tokeshi and T. Kitamori, *Anal. Chem.*, 2002, **74**, 1724.
- 26 B. Zhao, J. S. Moore and D. J. Beebe, *Science*, 2001, **291**, 1023.
- 27 B. Zhao, N. O. L. Viernes, J. S. Moore and D. J. Beebe, *J. Am. Chem. Soc.*, 2002, **124**, 5284.
- 28 L. Jiang and D. Erickson, *Small*, 2013, **9**, 107.
- 29 T. T. Huang, D. G. Taylor, M. Sedlak, N. S. Mosier and M. R. Ladisch, *Anal. Chem.*, 2005, **77**, 3671.
- 30 D. Huh, A. H. Tkaczyk, J. H. Bahng, Y. Chang, H. H. Wei, J. B. Grothberg, C. J. Kim, K. Kurabayashi and S. Takayama, *J. Am. Chem. Soc.*, 2003, **125**, 14678.
- 31 V. Srinivasan, V. K. Pamula and R. B. Fair, *Anal. Chim. Acta*, 2004, **507**, 145.
- 32 K. Handique, D. T. Burke, C. H. Mastrangelo and M. A. Burns, *Anal. Chem.*, 2000, **72**, 4100.
- 33 H. Andersson, W. van der Wijngaart, P. Griss, F. Niklaus and G. Stemme, *Sens. Actuators, B*, 2001, **75**, 136.
- 34 H. Andersson, W. van der Wijngaart and G. Stemme, *Electrophoresis*, 2001, **22**, 249.
- 35 S. H. Lee, C. S. Lee, B. G. Kim and Y. K. Kim, *J. Micromech. Microeng.*, 2003, **13**, 89.
- 36 Y. Y. Feng, Z. Y. Zhou, X. Y. Ye and H. J. Xiong, *Sens. Actuators, A*, 2003, **108**, 138.
- 37 Y. M. Zheng, X. F. Gao and L. Jiang, *Soft Matter*, 2007, **3**, 178.
- 38 T. Kim and K. Y. Suh, *Soft Matter*, 2009, **5**, 4131.
- 39 N. A. Malvadkar, M. J. Hancock, K. Sekeroglu, W. J. Dressick and M. C. Demirel, *Nat. Mater.*, 2010, **9**, 1023.
- 40 T. Q. Wang, X. Li, J. H. Zhang, X. Z. Wang, X. M. Zhang, X. Zhang, D. F. Zhu, Y. D. Hao, Z. Y. Ren and B. Yang, *Langmuir*, 2010, **26**, 13715.
- 41 T. Q. Wang, X. Li, J. H. Zhang, Z. Y. Ren, X. M. Zhang, X. Zhang, D. F. Zhu, Z. H. Wang, F. Han, X. Z. Wang and B. Yang, *J. Mater. Chem.*, 2010, **20**, 152.

ARTICLE

- 42 T. Gervais, J. El-Ali, A. Günther and K. F. Jensen, *Lab chip*, 2006, **6**, 500.
- 43 V. Nuñez, S. Upadhyayula, B. Millare, J. M. Larsen, A. Hadian, S. Shin, P. Vandrangi, S. Gupta, H. Xu, A. P. Lin, G. Y. Georgiev, and V. I. Vullev, *Anal. Chem.*, 2013, **85**, 4567.
- 44 S. Irandoust and B. Andersson, *Ind. Eng. Chem. Res.*, 1989, **28**, 1684.
- 45 A. Günther, M. Jhunjhunwala, M. Thalmann, M. A. Schmidt and K. Jensen, *Langmuir*, 2005, **21**, 1547.
- 46 H. R. Sahoo, J. G. Kralj and K. Jensen, *Angew. Chem. Int. Ed.*, 2007, **46**, 5704.
- 47 S. Hiki, K. Mawatari, A. Aota, M. Saito and T. Kitamori, *Anal. Chem.*, 2011, **83**, 5017.